16 Apr 2004, 8:00am - 9:30am

Numerical Modeling of Bistun Rock Slope Behavior in Grouting Using Discrete Element Method

S. Taghipoor
Amirkabir University of Technology, Tehran, Iran

S. A. Amirshahkarami
Amirkabir University of Technology, Tehran, Iran

H. Salari Rad
Amirkabir University of Technology, Tehran, Iran


Proceedings: Fifth International Conference on Case Histories in Geotechnical Engineering
New York, NY, April 13-17, 2004

Numerical Modeling of Bistun Rock Slope Behavior In Grouting Using Discrete Element Method

S. Taghipoor
Amirkabir University of Technology
Tehran, Iran

S.A. Amirshahkarami
Amirkabir University of Technology
Tehran, Iran

H. Salari Rad
Amirkabir University of Technology
Tehran, Iran

ABSTRACT

The discrete element method is an established method for considering discontinuous deformation behavior of joint systems. This paper provides a description of this algorithm used to model coupled hydraulic and mechanical effects of joints on rock mass behavior. The paper also describes Bistun rock slope stability analysis using empirical (SMR) and numerical (D.E.) methods. The behavior of the rock slope and rock blocks containing Bistun epigraph in grouting and groundwater flow has successfully simulated using UDEC (Universal Distinct Element Code) program. Finally, results have been presented and discussed on slope stability condition and grouting pressure.

INTRODUCTION

Hydromechanical behavior of jointed rock messes involves complex interactions between joint deformations and effective stresses, causing changes in aperture and thus, hydraulic conductivity. Since most of the rocks have low permeability, the hydraulic behavior of a rock mass is mainly determined by the jointing pattern which introduces a strong directional conductivity. Both hydraulic and mechanical behavior should be taken into account properly in any analysis procedure.
The distinct element method has enabled the analysis of discontinuous mechanical behavior of jointed rock since its introduction (Cundall, 1971). At the same time, several models for flow in fracture networks were developed and tested against laboratory-scale models (Louis, 1974, Wilson and Witherspoon, 1974, Wittke, 1970). However, General applicability of these flow models was limited by the assumption of constant joint aperture.
Early forms of the distinct element method were based on "cell-mapping" contact detection logic which did not permit consideration of flow in voids between blocks. In 1980, a new form of distinct element method was introduced (Cundall, 1980) in which the blocks were viewed as defining a network of interconnected voids and channels. The resulting code was called UDEC (Universal Distinct Element Code).
Early UDEC formulations were strictly limited to consideration of steady state confined flow. Nevertheless, essential features of Hydromechanical behavior were computed, allowing unprecedented analysis of important engineering problems.
Fairhurst and Lemos (1988) used UDEC to study the influence of joints in rock on water losses in pressure tunnels and the validity of the hydraulic fracturing test as an indicator for determining the need to line such tunnels. The main purpose of their studies was to develop a reasonable phenomenological understanding of the problem.
Analysis of flow in jointed rock beneath concrete gravity dams are reported by Lemos (1987). These studies focused on the dynamic behavior of such dams, including the effects of water pressure in joints. Numerical simulations using a continuously-yielding joint model show how repeated occurrences of dynamic events can progressively degrade the stability of the structure.
Brady (1989) reports the use of a flow model using a Bingham substance to study the penetration of cement-based grouts in jointed rock. The introduction of this fluid model (in which no flow occurs until a threshold pressure gradient is overcome) into UDEC takes account of the pronounced pressure dependence of grout flow properties.

FUNDAMENTAL OF DISCRETE ELEMENT METHOD

Formulation

In this section, the current fluid flow formulation used in UDEC is presented. The program UDEC has the capability to model the flow of a fluid through the fractures of a system of impermeable blocks. A fully coupled mechanical-hydraulic analysis is performed in which fracture conductivity is dependent on mechanical deformation and in which joint water pressures are taken into account in the mechanical computations. At present, both confined flow and flow with a free surface can be considered. An efficient algorithm has

been developed for steady state problems, but transient analysis can also be performed.

The numerical implementation makes use of the particular methodology adopted in this code for the presentation of a two dimensional of closely packed discrete blocks (Cundall, 1980). The blocks are viewed as defining a network of interconnected voids and channels that will be referred as "domains". Referring to Fig. 1, domains are numbered 1 to 5. Domains 1, 3 and 4 represent joints, domain 2 is located at the intersection of two joints, and domain 5 is a void space. Domains are separated by the contact points (designated by letters A to F in Fig. 1), which are the points where the forces of mechanical interactions between blocks are applied. Deformable blocks are discretized into a mesh of triangular (uniform stress) elements. Gridpoints may thus exist not only at the vertices of the blocks, but also along the edges. A contact points will be placed wherever a gridpoints meets an edge or a gridpoint of another block. For example, in the same figure, contact D implies the existence of a gridpoint along one of the edges in contact. As a consequence, the joint between the two blocks is represented by two domains: 3 and 4. If a finer internal mesh were adopted, the joint would be represented by a larger number of contiguous domains. Therefore, the degree of refinement of the numerical representation of the flow network is linked to the mechanical discretization adopted, and can be defined by the user.

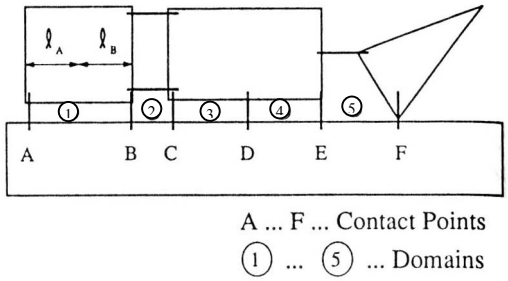

Fig. 1. Figure showing definition of domains used in UDEC

In the absence of gravity, a uniform fluid pressure is assumed to exist within each domain. For problems with gravity, the pressure is assumed to vary linearly according to the hydrostatic gradient, and the domain pressure is defined as the value at the center of the domain.

Flow is governed by the pressure differential between adjacent domains. The flow rate is calculated in two different ways, depending on the type of contact. For a point contact (i.e. corner-edge, as contact F in Fig. 1, or corner-corner), the flow rate (from a domain with pressure p_1 to a domain with pressure p_2) is given by:

$$q = -k_c \Delta p \tag{1}$$

Where k_c is a point contact permeability factor and

$$\Delta p = p_2 - p_1 + \rho_w g(y_2 - y_1) \tag{2}$$

Where ρ_w is the fluid density, g is the acceleration of gravity (assumed to act in the negative y direction), y_1 and y_2 are the coordinates of the domain centers.

In the case of an edge-edge contact, a contact edge can be defined, (e.g. in Fig. 1, l_A and l_B denote the length of contacts A and B, respectively). In this case, the cubic law for flow in a planar fracture (e.g., Witherspoon et al., 1980) can be used. The flow rate is then given by:

$$q = ba^3 \Delta p / l \tag{3}$$

Where b is a joint permeability factor (whose theoretical value is $1/12\mu$, μ is the dynamic viscosity of the fluid), a is the contact hydraulic aperture and l is the length of contact between the domains.

In UDEC, the user may prescribe the factor b, and select and exponent different from 3. The above expression may also be used for point contacts provided a minimum length is assigned to these contacts.

The hydraulic aperture is given, in general, by:

$$a = a_0 + u_n \tag{4}$$

Where a_0 is the joint aperture at zero normal stress, and u_n is the joint normal displacement (positive denoting opening) A minimum value, a_{res}, is assumed for the aperture, beyond which mechanical closure does not affect the contact permeability. (The above expression is a very simple relation between joint mechanical and hydraulic apertures) The program UDEC employs an explicit time stepping scheme for the solution of the equations of motion of the system. This dynamic algorithm also allows the solution of quasi-static problems by introducing viscous damping, as in the dynamic relaxation method (Otter et al. 1966).

At each timestep, the mechanical computations determine the geometry of the system, thus yielding the new values of apertures for all contacts and volumes of all domains. Flow rates through the contacts can then calculated based on the above formulas. Then, domain pressure are upgraded, taking into account the net flow into the domain, and possible changes in domain values due to the incremental motion of the surrounding blocks. The new domain pressure becomes:

$$p = p_0 + K_w Q \Delta t / V - k_w \Delta V / V_m \tag{5}$$

Where p_0 is the domain pressure in the preceding time step, Q is the sum of flow rates into the domain from all surrounding contacts, K_w is the bulk modulus of the fluid and

$$\Delta V = V - V_0 \qquad , \qquad V_m = (V + V_0)/2$$

Where V and V_0 are the new and old domain areas, respectively.

Given the new domain pressures, the forces exerted by the fluid by the edges of the surrounding blocks can be obtained. These forces are then added to the other forces to be applied to the block gridpoints, such as the mechanical contact forces and external loads. As a consequence of this procedure, total stresses will result inside the impermeable blocks, and effective normal stresses will be obtained for the mechanical contacts. Numerical stability of the present explicit fluid flow algorithm requires that the time step be limited to:

$$\Delta t = \min\left[V \Big/ \left(K_w \sum_i k_i \right) \right] \tag{6}$$

Where V is domain volume, and the summation of permeability factors k_i is extended to all contacts surrounding the domain.

For example, when the cubic flow law is used, this factor is given by:

$$k_i = \frac{ba^3}{l} \tag{7}$$

The minimum value of Δt for any domain is used in the analysis.

For transient flow analysis, the numerical stability requirements may be rather severe, and may make some analyses very time consuming or impractical, especially if large contact apertures and very small domain areas are present. A scheme that can be used to enhance computational efficiency consist in assigning to domains at the intersections of the joints part of the volume of the joints meeting at that point, and correspondingly reducing the volume of the joint domains. Furthermore, the fluid filling a joint also increases the apparent joint stiffness by K_w/a, thus possibly requiring a reduction of the timestep used in the mechanical calculation.

In many studies, only the final steady state condition is of interest. In this case, several simplifications are possible which make the present algorithm very efficient for many practical problems. The steady state condition does not involve the domain volumes. These can thus be scaled to improve the convergence to the solution. A scheme that was found to produce good results consist in Assigning to a given domain volume V that inserted in the time step expression above leads to the same timestep for all domains. The contribution of the change in domain volume to the pressure variation can also be neglected, thus eliminating the influence of the fluid stiffness in the mechanical timestep. Furthermore, as the steady state condition is approached, the pressure variation in each fluid step becomes very small, allowing the execution of several fluid steps for each mechanical step without loss of accuracy. An adaptive procedure was implemented in UDEC, which "triggers" the update of the mechanical quantities, whenever the maximum increment of pressure in any domain exceeds some prescribed tolerance (for example, 1% of the maximum pressure).

Visco-Plastic Flow in Joints

The flow of a Bingham body (or liquid) such as cement grout is of the visco-plastic type. The major difference between this model and that for a Newtonian liquid is that, for a Bingham fluid, a yield stress, τ_y, must be exceeded to initiate flow.

For Newtonian flow, it is assumed that the flow rate per unit width, q, is related linearly to the pressure gradient, J, as shown in Fig. 2. The general equation for fluid flow between planar surfaces is given by:

$$q = \frac{ba^x J}{12\mu} \tag{8}$$

Where a = fracture width (aperture), b = empirical coefficient, μ= dynamic viscosity of fluid, and x = aperture exponent.

In the most widely used form of this relation, known as the cubic flow law, x = 3 and b = 1. The flow gradient relation of a Bingham body is similar, except that no flow occurs until the threshold gradient, J_0, is exceeded, as shown in Fig. 3.

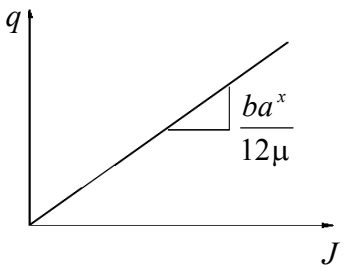

Fig. 2. Flow-gradient relation for Newtonian fluid in UDEC

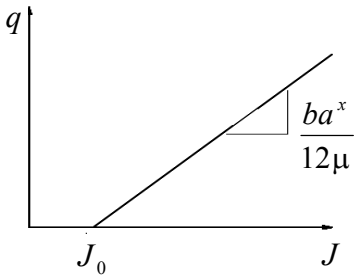

Fig. 3. Flow-gradient relation for Bingham fluid in UDEC

Considering the balance of forces on a rectangular element of fluid, the expression for the threshold gradient for flow between parallel sides of aperture, a, is given by:

$$J = \frac{2\tau_y}{a} \tag{9}$$

The expression for the threshold gradient can also be obtained by considering the equation for steady laminar flow of a Bingham plastic in a circular pipe. This equation is known as Buckingham's equation (Wilkinson, 1960):

$$Q = \frac{\pi r^4 \Delta P}{8L\mu_p}\left[1 - \frac{4}{3}\left[\frac{2L\tau_y}{r\Delta P}\right] + \frac{1}{3}\left[\frac{2L\tau_y}{r\Delta P}\right]^4\right] \tag{10}$$

Where Q = volume rate of flow, r = pipe radius, μ_p = Bingham plastic viscosity, ΔP/L = pressure gradient = J, and τ_y = yield stress.

From this expression, it can be seen that no flow occurs if the pressure gradient J is zero or equals $2\tau_y/\gamma$. It is not clear from the equation what occurs at pressure gradients between zero and$2\tau_y/\gamma$, but it is reasonable to assume that no steady flow occurs within this range. Therefore, the threshold gradient, J_0, the gradient at which steady flow is possible, is given by:

$$J_0 = \frac{2\tau_y}{r} \tag{11}$$

Note that this expression can also be derived by considering the balance of forces acting on a cylindrical element of fluid with radius r and length L.

BISTUN EPIGRAPH

Bistun Epigraph has been lithographed in 500 B.C. at the age of Hakhamaneshian by the order of Daryoosh. The epigraph is located on a rock slope at the 30th km of Kermanshah-Hamedan road, at a height of 40 m from the road level. Due to

the fact that the epigraph is an evidence of Hakhamaneshi age, it holds an exceptional importance with respect to other historic epigraphs. It gives priceless information about the rules and the way of living in the age of Hakhamaneshian.

GEOLOGY AND MORPHOLOGY

The rock slope including Bistun epigraph has a 120 meters height with vertical slope face on which the epigraph has been placed (at height of 40 m). This slope is a part of a V shaped gap, which is made by the adjacent fault (Fig. 4). The fault has a north-south strike.

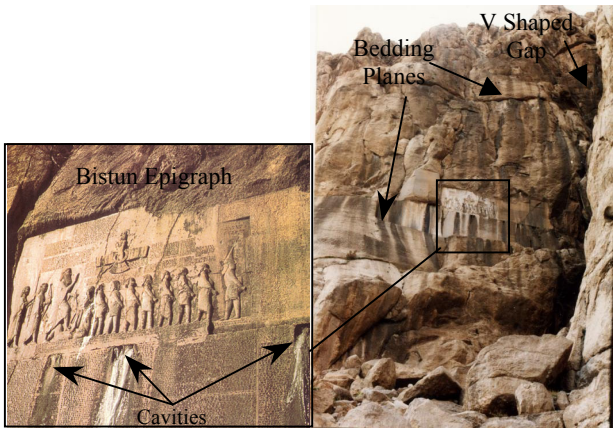

Fig. 4. Bistun epigraph and rock slope

The slope rock mass is composed of massive microcrystalline limestone which belongs to lower Cretaceous and upper Jurassic. Microscopic and field investigations showed that tectonic stresses were applied to the rock mass in the past due to neighboring of active tectonic subduction zone (Bistun limestone and Kermanshah Ophiolites). As a result, fissures and fractures have been extended in the rock mass extensively. In the next stage, placement of rock mass in water media resulted in filling the fissures and fractures with calcite (uniaxial and triaxial tests confirm this phenomena). So the filling calcite is the only factor in providing the strength of intact rock and rock mass and consequently, if the calcite vanishes due to water activity, serious situation takes place to the rock slope and the Bistun epigraph.

To study the discontinuities, dip and dip direction of discontinuities with extension greater than 1 meter have been logged using scan line method in a radius of 1 km at the center of the epigraph. The data was processed using the Schmitt net. Results and other parameters have been listed in table 1. The Bistun rock slope has a vertical slope face with dip direction and dip of about 100/90. Figure 5 illustrates the rock slope and the discontinuities.

Based on above stated studies, it seems that the precipitations percolating in rock mass, flow to Bistun Epigraph by means of two-bedding planes (Fig. 6). The beddings have aperture of about 1 to 2 millimeters due to solubility of precipitations containing CO_2. Furthermore, the beddings have slow dip to the epigraph. The above-mentioned process has generated the cavities shown by Fig. 4.

Table 1. Discontinuity characteristics of Bistun rock slope

Type of Discontinuity	Dip Direction (deg.)	Dip (deg.)	Spacing (m)	JRC_{100}	Aperture (mm)
Joint set 1	114	90	1-2	9	0.1
Joint Set 2	190	80-90	3-5	9	0.1
Bedding Plane	109	12	1	2.3	1-2
Random Joint Set 3	43	58	---	---	---
Random Joint Set 4	151	71	---	---	---

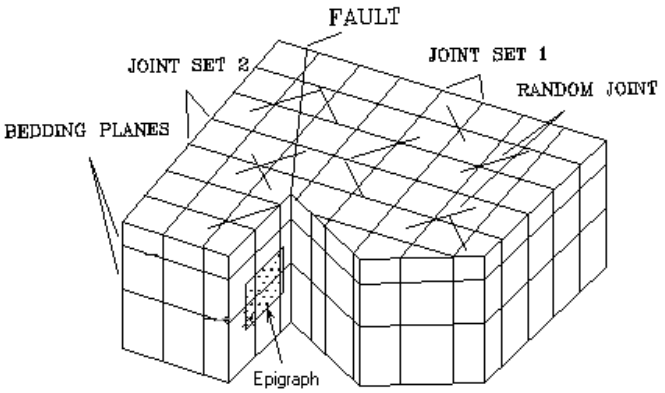

Fig. 5. Schematic view of Bistun rock slope and its discontinuities

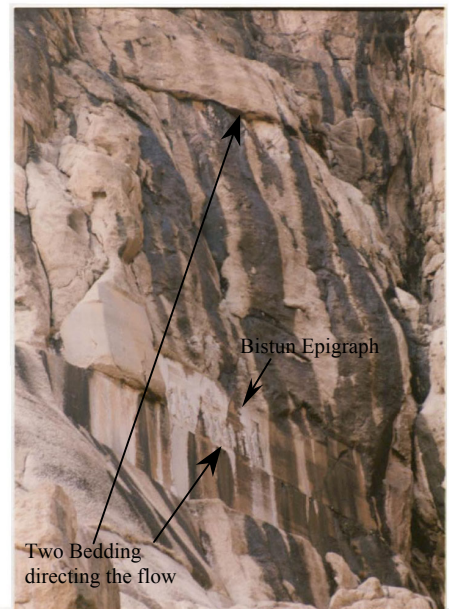

Fig. 6. Ground water flows into the epigraph by means of two beddings

LABORATORY TESTS ON INTACT ROCK

Uniaxial, triaxial and Brazilian tests have been carried out on intact rock samples of Bistun rock slope in Rock Mechanics Laboratory of Amirkabir University of Technology. The results have been listed in table 2. One should note that in the uniaxial tests, the planes of failure follow the pattern of fractures and micro fractures filled with calcite composing texture of Bistun limestone. In some samples, thickness of fillings reaches 10 millimeters (Fig. 7).

Table 2. Results of laboratory tests on intact rock samples of Bistun limestone

Uniaxial Compressive Strength (MPa)	Uniaxial Tensile Strength (MPa)	Elastic Modulus (GPa)	Poison Ratio	Cohesion (MPa)	Internal Friction Angle (Degree)	N_ψ^*	m^{**}
30	4.5	5.7	0.3	8.5	30	3	4.86

* Constant in Mohr-Coulomb criterion
** Material constant in Hoek-Brown criterion

Fig. 7. Calcite filling fractures and fissures of intact rock controlling the plane of failure

ROCK MASS CLASSIFICATION

SMR System

In order to evaluate the stability of rock slopes, a classification system was proposed which called Slope Mass Rating System (SMR)(Taghipoor, 2003). Slope Mass Rating is obtained from Bieniawski's Rock Mass Rating (RMR) by subtracting adjustment factors of the joint-slope relationship and adding a factor depending on method of excavation:

$$SMR = RMR_{basic} - (F_1.F_2.F_3) + F_4 \qquad (12)$$

Where RMR_{basic} is evaluated according to Bieniawski (1979, 1989) by adding the ratings of corresponding five parameters. The F_1, F_2 and F_3 are adjustment factors related to joint orientation with respect to slope orientation and F_4 is the correction factor for the method of excavation. The SMR value of the rock slope including Bistun epigraph has been estimated about 58. So the rock mass is placed in class III (normal slope mass). According to SMR classification system, planar and wedges failures can occur in class III rock mass. Many remedial measures can be taken to support a slope. Both detailed study and good engineering sense are necessary to stabilize a slope. Classification systems can only try to point the normal techniques of support. According to SMR classification, suggested supports for class III are: Toe ditch and/or nets, spot or systematic bolting, spot shotcrete.

GSI System

Hoek E. And Brown E.T. (1997) introduced the Geological Strength Index, GSI, for both hard and weak rock masses. Experienced engineers and geologists generally show tendency to a simple, fast and yet reliable classification, which is based on visual inspection of geological conditions. Most of the researchers suggest that a classification system should be nonlinear for poor rocks as strength deteriorates rapidly due to weathering. Furthermore, increasing application of computer modeling has created an urgent need for a classification system tuned specially for simulation of rock structures. To meet other needs, Hoek E. And Brown E.T. (1997) devised simple charts for estimating GSI based on the following two correlations:

$$GSI=RMR-5 \quad \text{for GSI>18 or RMR>23} \qquad (13)$$

Where RMR is the Rock Mass Rating according to Bieniawski (1989).
Based on RMR for the Bistun rock mass, which has been evaluated about 63 to 68, GSI will be in the range of 58-63 (average 60.5). According to GSI classification, the rock mass properties of Bistun rock slope will be as shown by table 3.

Table 3. Strength and deformation characteristics of Bistun rock mass

Parameter	Value
Uniaxial Compressive Strength (MPa)	4
Uniaxial Tensile Strength (MPa)	0.53
Deformation Modulus (GPa)	3
Poison Ratio	0.3
Cohesion (MPa)	1.8
Internal Friction Angle (degree)	30
Dilation Angle (degree)	4
m^*	0.82
s^{**}	0.012

*, ** are material constant in Hoek and Brown criterion

NUMERICAL ANALYSIS

Till now, it has been shown that the only problems are hydromechanical effects of precipitations percolating to rock slope as a matter of structural fractures. The water has carbon

dioxide and hence can solve limestone easily. Therefore, the water can solve the calcite filling the fractures and surface of bedding planes. This is why the bedding planes have become hydraulic paths by which groundwater flows to the slope face and epigraph.
Now, two ways are considered to protect the epigraph: 1. Drainage and 2. Grouting. It is obvious that drainage cannot deviate all of the groundwater and can only decrease it. Thus, grouting and execution of a sealing curtain behind the epigraph is highlighted. By this way, the water behind the curtain must be drained to decrease the water pressure.
Grouting pressure can make the slope unstable. A small slide of a block around the epigraph can hurt the epigraph irrecoverably. So, the final aim of numerical modeling in this paper is to determine the safe grouting pressure.

Hydromechanical Analysis of Underground Water

A model has been prepared to evaluate the water flow pattern in the fracture system of the rock slope. In this model, we assumed that the ground water reach the top of the slope at a distance of 80 m rare of the slope face. The result shows that the flow rate is in maximum value of about 90 lit/min in the outlet of the bedding plane (in the middle of the epigraph, Fig. 8). At this point, several cavities can be seen which confirm the results. Moreover, the water pressure behind the epigraph is about 44 kPa.

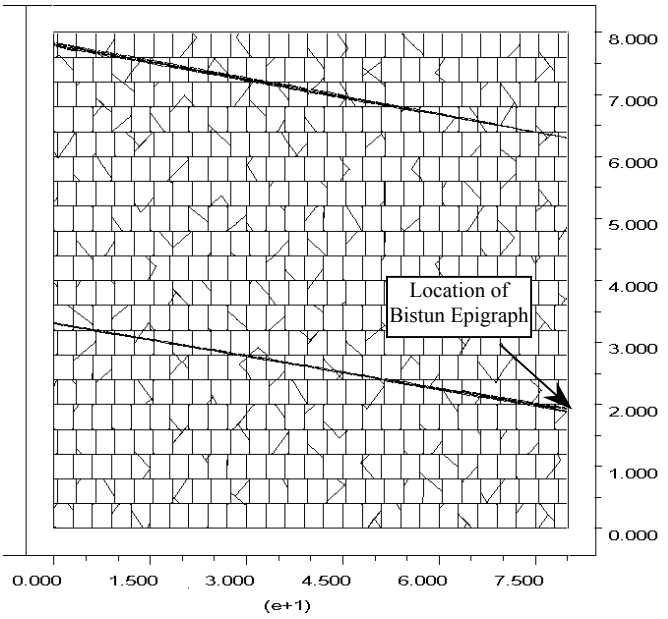

Fig. 8. Flow rates in natural groundwater model (The line thickness is proportional to the flow rate; max. flow=1.609e^{-3} m^3/sec; flow rates less than 3.218e^{-4} m^3/sec not shown)

Hydromechanical Analysis of Grouting

These models concern grouting pressure and the effect of grouting on stability of the rock slope. We tried to determine the maximum safe grouting pressure using discrete element method. Furthermore, to increase grouting pressure and the effective penetration radius of grout, we have used two rows of rock bolts. The borehole diameter is 100 mm in all models.
The grout characteristics are based on the behavior of suspension cement grouts, which have been listed in table 4. Cement grouts act like a Bingham fluid.
Change in grouting pressures, position of grout borehole and existence of rock bolts make the grouting models different.

Table 4. Behavior and strength characteristics of cement grout used in DEM analysis (Kutzner, 1996)

Compressive strength after 28 days (MPa)	Sedimentation DH/H^6 (%)	Flow Limit (Pa)	Viscosity (s.MPa)	Unit Weight (KN/m^3)	Water/solid ratio	Cement (Kg)	Water (lit.)
10	40	0.5	6	14	1.5	50	100

In the first model, the grouting borehole is placed at 4 meters behind the epigraph and on the bedding surface (Fig 9). As a thumb rule, 0.1 bar grouting pressure is considered for every 10 m overburden (Kutzner, 1996). The epigraph level has 80 meter overburden. So, initially, 0.8 bar pressure is appropriate for grouting. Therefore grout pressure equal to 1 bar (in five 0.2-bar cycles) has been applied to borehole perimeter in DEM model (In all models, the final pressure has been applied in five cycles). Due to high aperture of the bedding plane, grout could flow to adjacent joints. The distribution of grout pressure in joints (Fig. 9) shows that grout pressure reaches 1.3 bar in the joint behind the epigraph. If the grout load applied to the blocks including the epigraph becomes greater than frictional strength, the epigraph will move. Figure 10 shows the distribution of block displacements surrounding the epigraph. Displacements of block including the epigraph vs. artificial time have been monitored in model, which is shown in Fig. 11. According to the results, if the grouting borehole is drilled at 4 m behind the epigraph, grouting at 1 bar pressure will be safe. Increase of pressure in the same model yields to instability.
In the next models, the grouting borehole is placed at 8 meters rare of the epigraph, on the bedding surface. Pressure in range of 1 to 4.5 bar have been applied and analyzed. Results show that 1.5 bar will be safe and pressures more than this will make the epigraph unstable. Some other models were presented to increase grouting pressure. We used two rows of horizontal (dip 0 degree) rock bolts with the length of 10 meters above and under the bedding (epigraph) (Fig. 12). The rows have 4 meters spacing. Several grouting pressures have been applied to determine the safe grouting pressure. In this condition, models show that maximum safe grouting pressure is about 2 bar. The tensile loads in rock bolts have been shown in Fig. 12.
By changing the length and dip of rock bolts, several other models were checked. The results have been presented in table 5. For the optimal condition, the length and dip of rock bolts

and grouting pressure will become 10 meters, 10 degree (with respect to horizon) and 2.5 bar, respectively.

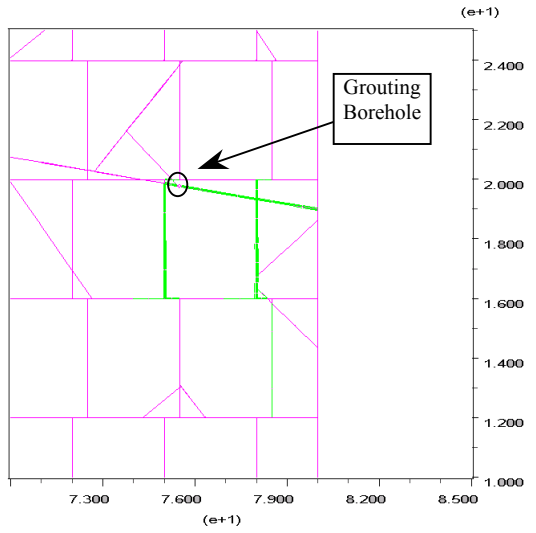

Fig. 9. Domain pressures in grouting (The line thickness is proportional to the domain pressures; max. pressure =137.6KPa; pressures less than 27.51 KPa not shown)

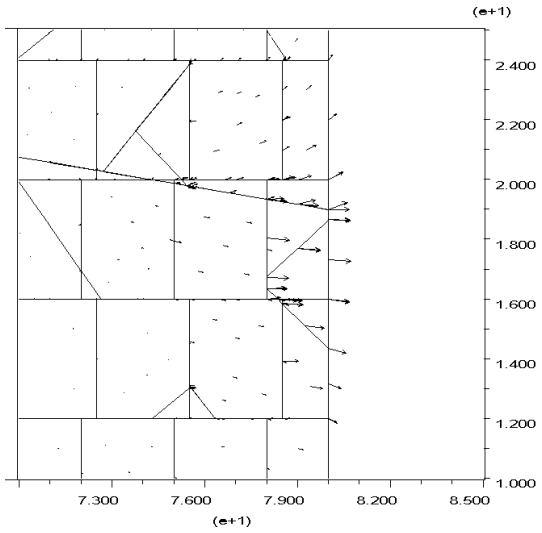

Fig. 10. Distribution of displacements in grouting at pressure 1 bar (Max. displacement= 0.52 mm at equilibrium)

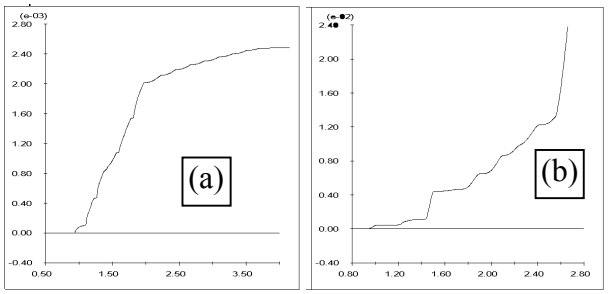

Fig. 11. Graph of displacement vs. artificial time for block including Bistun epigraph in grouting at pressure (a) 1 bar, (b) 2 bar, grouting borehole at 4 m from epigraph

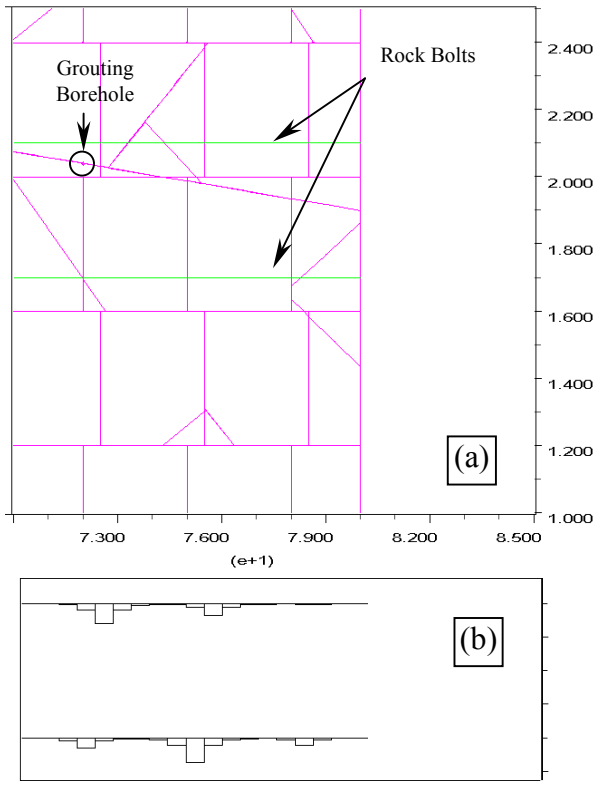

Fig. 12. Rock bolts (a) and axial loads (b) in them during grouting at 2 bar. Maximum axial load is equal to 160000 N.

Table 5. Results of DEM analysis of grouting process

Distance Between Grouting Borehole and the Epigraph (m)	Two Rows of Rock Bolts	Safe Grouting Pressure (bar)	Length of Rock bolts (m)	Dip of Rock Bolts with respect to horizon (deg.)*
4	--	1	--	--
8	--	1.5	--	--
8	Exist	2	10	0
8	Exist	2.5	10	10
8	Exist	2	10	30
8	Exist	1.9	6	0
8	Exist	2	6	10
8	Exist	1.5	6	30

* For the upper row is positive and for the lower is negative

Numerical models indicated that maximum safe grouting pressure could reach 2.5 bar in the existence of optimal rock bolts. However, we suggest that grouting in this condition be performed at pressure 1.5 bar since the errors and uncertainties due to uncontrollable problems, tools, apparatus and labor should be considered. Furthermore, instrumentation and monitoring is essential during grouting.

SUMMARY AND CONCLUSION

Investigations and studies have been performed on Bistun epigraph and rock slope and problems have been founded and discussed. Finally, to execute a grouting curtain, several numerical models were prepared and final safe grouting pressure is determined. The results of the study are as follow:

1. The rock slope has 2 main joint set and random joints and a set of bedding plane. A bedding plane is connected to the middle of the epigraph, has low dip to the slope face (epigraph). So, the bedding has become a hydraulic path, which lead the ground water to the Bistun epigraph and makes several cavities in the intersection of bedding and slope face.
2. Laboratory tests including uniaxial and triaxial compression tests confirm the microscopic results about filling of fractures and fissures by calcite. The filled fractures control the strength of intact rock and rock mass.
3. Hydromechanical numerical models showed that maximum ground water flow is in the outlet of bedding in the middle of epigraph. Several cavities in field investigation verify this fact.
4. It seems that execution of a sealing curtain behind the epigraph is effective to prevent the water from flowing into the epigraph.
5. Models prepared by UDEC showed that in the absence of rock bolts, when grouting borehole is drilled in 4 and 8 m behind the epigraph on the bedding plane, grouting pressures of 1 and 1.5 bar would be safe, respectively.
6. Grouting pressure can increase if two rows of rock bolts are used. In the optimum condition, rock bolt length and dip are about of 10 m and 10 degrees, resulting in the maximum grouting pressure of 2.5 bar.

ACKNOWLEDGEMENT

We would like to thank Dr. D Reyeesi G. for software supporting, Mrs. M. Mehdi Abadi for several useful discussions and field investigations, and the faculty of Amirkabir University of Technology. The assistances of Mr. R. Taghipoor and Mr. H. Abbasi in final editing are gratefully acknowledged.

REFFERENCES

Barton, N., S. Bandis and K. Bakhtar [1985], "Strength, deformation and conductivity coupling of rock joints", Int. J. Rock Mech. Sci. Vol., 22 pp.121-140.

Bieniawski, Z.T. [1979], "The Geomechanics Classification in Rock Engineering Applications", Reprinted from: Proc. 4th Cong. Of the Int. Society for Rock mech., 3 Vols., Balkema, Rotterdam, Netherland.

Bieniawski, Z.T. [1989], "*Engineering Rock Mass Classification*", John Wiley, p.251.

Brady, B.H. [1989], "Rock mechanics and ground control for underground mining and construction" *Rock Mechanics as a Guide for Efficient Utilization of Natural Resources*, pp. 5-18, Rotterdam, Balkema.

Cundall, P.A. [1971], "A computer model for simulation progressive large scale movements in blocky rock systems", *Proc. Symp. Int. Soc. Rock Mech., Nancy France*, Vol. 1, Paper No. II-8.

Cundall, P.A. [1980], "UDEC-A generalized distinct element program for modeling jointed rock", *Final Technical Report, European Research Office*, U.S. Army.

Fairhurst, C., and J.V. Lemos [1988], "Influence of in-situ stresses on fluid penetration in jointed rock from unlined pressure tunnels", *Proc. Symp. Rock Mech. & Power Plants*, Madrid.

Hoek E. And E.T. Brown [1997], "Practical Estimates of Rock Mass Strength", *Int. Jr. Rock Mech. And Mining Sci.*, Pergamon, Vol. 34, No. 8, pp. 1165-1186.

Kutzner C. [1996], "*Grouting of Rock and Soils*", Balkema, Rotterdam, Brookfield, p. 271.

Lemos, J.V. [1987], "A distinct element model for dynamic analysis of jointed rock with application to dam foundations and fault motion", *Ph.D. Thesis*, University of Minnesota, Minneapolis.

Louis, C. [1974], "Rock Hydraulics", *Rock Mechanics*, Germany, University of Carlsruhe, pp. 229-387.

Otter, J.R.H., A.C. Cassell and R.E. Hobbs [1966], "Dynamic Relaxation", *Proc. Inst. Civil Engrs*., 35: 633-665.

Wilson, C.R. and P.A. Witherspoon [1974], "Steady state flow in rigid networks of fractures", *Water Resources research*, Vol. 10(2), pp. 328-335.

Taghipoor, S. [2003], "Hydromechanical Numerical Analysis of Bistun Epigraph and Stabilization", *MSc. Thesis*, Amirkabir University of Technology, Tehran.

Wilkinson, W. L. [1960], "Non-Newtonian Fluids", *Fluid Mechanics, Mixing and Heat Transfer*, London: Pergamon Press.

Witherspoon, P.A., J.S.Y. Wang, K. Iawi and J.E. Gale [1980], "Validation of cubic law for fluid flow in a deformable rock fracture", *Water Resources research*, Vol. 16, pp. 1016-1024.

Wittke, W. [1970], "Tree dimensional penetration in fissured rock", *Proc. Open Pit Mining Symp*., Johannesburg, pp. 181-191.